


Cite this: *RSC Adv.*, 2015, 5, 21495

Synthesis, chiroptical and SHG properties of polarizable push–pull dyes built on π -extended binaphthyls†

Carmine Coluccini,^a Marco Caricato,^a Elena Cariati,^{bc} Stefania Righetto,^b Alessandra Forni^c and Dario Pasini^{*ad}

We report on new enantiopure binaphthyl derivatives in which electron-donating and electron-withdrawing substituents are placed in direct conjugation, to create active push–pull dyes for NLO applications. The dyes, unprecedentedly, extend their π -bridge from the 3,3' positions of the binaphthyl units, and incorporate as acceptors pyridine units, possessing a coordinating nitrogen atom useful for further supramolecular polarization of the chiral dyes. The π -bridge is constructed by the sequential attachment of phenylenevinylene units to the enantiopure binaphthyl derivatives through Horner–Wadsworth–Emmons olefination, which proceed with high stereoselectivity, affording stereodefined chiral dyes. The polarization of the terminal pyridine units by means of labile complexation with Pd^{2+} ions has been demonstrated using both optical and chiroptical methods. The polarization by protonation can be made reversible in solution and solid state by exposure to ammonia vapors, as shown by absorption and emission spectroscopies. NLO properties, as determined by EFISH generation measurements in solution, are significant for the bisprotonated species when compared to previously reported binaphthyl substrates. TDDFT calculations show that the hyperpolarizability tensor contribution is responsible for enhancing SHG values upon protonation up to one order of magnitude, highlighting the potential of such *ortho* related, axially-chiral push–pull dyes for functional NLO applications.

Received 22nd December 2014
Accepted 19th February 2015

DOI: 10.1039/c4ra16876c

www.rsc.org/advances

Introduction

Conjugated organic materials are currently used or being developed for a number of technological applications. Amongst these, well-defined π -extended organic oligomers have been the subject of increasing attention in the last few decades, either in solution or in bulk. Their utility as model structures for the understanding of the solution and bulk scale properties of conjugated polymers should also be stressed.¹ One of the most prominent examples of the application of conjugated organic molecules is in the field of second harmonic generation (SHG),² a nonlinear optical property which is at the foundation for advanced technologies in materials science and biological imaging. SHG is forbidden in the presence of a centrosymmetric

material; chiral organic molecules, by definition non-centrosymmetric, have thus been widely studied as materials capable of SHG.²

Chirality can play a fundamental role in tuning the properties of nanoscale structures, and of matter in general; in addition, nanostructuring *via* self-assembly of the chiral organic dyes has been shown to have pronounced effects and amplifications of their SHG response.³ Amongst known atropoisomeric chiral compounds, binaphthyls play a preeminent role, but applications of these compounds in the field of nanosciences are recent, and not yet fully explored.⁴ Typical efficient organic π -conjugated chromophores for SHG are “push–pull” in nature, bearing both electron-withdrawing and electron-donating organic functionalities in direct conjugation with each other, by means of an extended conjugated bridge with delocalized π -electrons.

Binaphthyl compounds have been exploited for the realization of second-order nonlinear optical (NLO) materials, having the combined advantages of being chromophores, and carrying the required element of chirality for bulk anisotropy.⁵ In fact, several organic molecular modules have been reported in which electron donating substituents in the 2,2' positions of the binaphthyl skeleton (dialkoxy substituents, such as in compound 1 (ref. 6) in Fig. 1, or dialkylamino substituents, such as in compound 2 (ref. 7) in Fig. 1) have their counterpart

^aDepartment of Chemistry, University of Pavia, Viale Taramelli 10, 27100 Pavia, Italy. E-mail: dario.pasini@unipv.it

^bDipartimento di Chimica dell'Università degli Studi di Milano, UdR dell'INSTM, via Golgi 19, 20133 Milano, Italy

^cIstituto di Scienze e Tecnologie Molecolari – Consiglio Nazionale delle Ricerche (ISTM-CNR), Università degli Studi di Milano, UdR dell'INSTM, via C. Golgi 19, 20133 Milano, Italy

^dINSTM Research Unit, University of Pavia, Italy

† Electronic supplementary information (ESI) available: Additional NMR spectra, absorption and emission spectra, and computational details, copies of NMR and mass spectra of newly synthesized compounds. See DOI: 10.1039/c4ra16876c



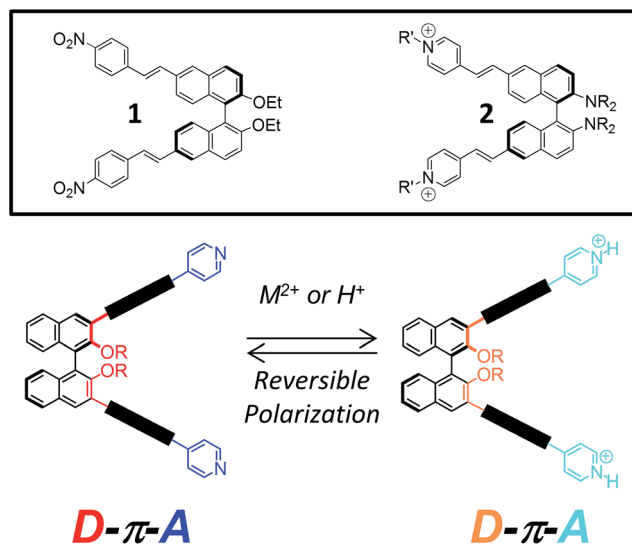


Fig. 1 Known, representative examples of functionalized binaphthyls for SHG (top), and design of novel 3,3'-binaphthyl disubstituted synthons displaying reversible coordination at the pyridine nitrogen atoms.

in the electron-withdrawing substituents placed at the most electrophilic 6,6' position (Fig. 1, top). Pyridines, being electron-poor heterocycles, can be ideal "pull" end moieties, when in direct π -conjugation with other "push" functionalities, for the preparation of efficient SHG chromophores: in fact, as an additional feature, they can be coordinated to their nitrogen atom, and their "pull" electronic character is in this case further enhanced.⁸ This coordination can be either irreversible (covalent functionalization, as in compound 2) or reversible, by means of weak coordination with a metal cation, protonation, supramolecular complexation through halogen bonding.⁹ The reversible protonation of the pyridinic moiety has recently resulted in interesting switchable emissive and non linear optical (NLO) materials.¹⁰ In addition to compound 2, several other pyridine-binaphthyl π -conjugated systems have been reported, branching out from the 3,3' or 6,6'-positions of the binaphthyl skeleton, for elegant applications in the field of metal-organic frameworks, or metallamacrocycles.¹¹

The substitution pattern can be amongst the various factors, which include weak intramolecular interactions, buttressing effects by sterically hindered substituents in vicinal positions, and at the supramolecular level, packing effects in crystals, which can have a profound effect on the dihedral angle between the naphthyl units of the binaphthyl moiety. Given our previous synthetic work with binaphthyl compounds derivatized at the 3,3' positions,¹² and our recent realization of crescent, push-pull, PPV-like chromophores,¹³ we present here the synthesis of novel enantiopure binaphthyls, in which pyridyl substituents branch out from the 3,3' positions of the binaphthyl skeleton (Fig. 1, bottom). Here we discuss on the chiroptical properties associated with complexation of the pyridine nitrogen atoms to Pd²⁺ ions and on the modulation of the optical behavior using acidic vapor as an external trigger.

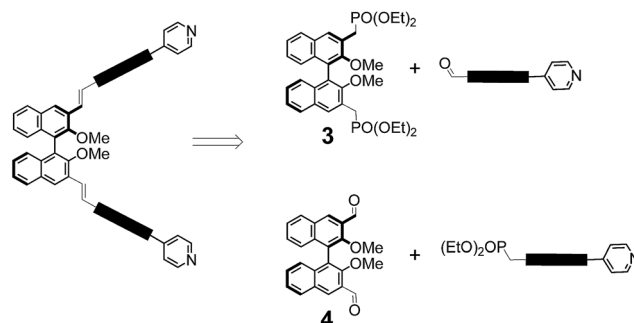
Results and discussion

Synthesis of the molecular modules

In our design strategy (Fig. 1, bottom), the electron-donating -OR substituents are in an *ortho* relationship with respect to the growing π -bridge in the 3,3' position, achieving efficient conjugation with the π -bridge and charge transfer with the electron-withdrawing unit since resonance delocalization of π -electrons is feasible. The synthetic approach makes use of a convergent approach for the instalment of pyridine endcapping functionalities, and of Horner-Wadsworth-Emmons (HWE) olefination reactions for the efficient and highly stereoselective formation of conjugated double bonds within the π -bridge.^{13a}

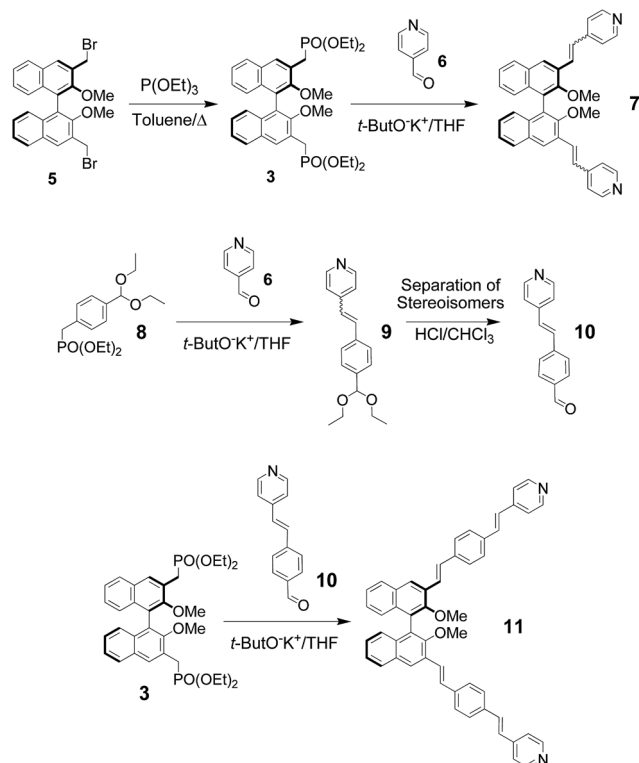
Amongst the two possible retrosynthetic approaches for the construction of the envisaged molecules, we used a difunctional phosphonate binaphthyl derivative (compound 3 in Scheme 1), in combination with π -extended pyridylaldehydes in HWE olefination reactions. In fact, previous work in our laboratories on similar substrates had revealed that the complementary approach, that is, the use of dialdehyde 4 in combination with a π -extended benzyl pyridyl phosphonate is not viable, since decomposition occurs in the presence of the strong bases required for HWE reactions, when carbon-carbon double bonds are present in the π -extended structures.

The synthesis of the key compounds is shown in Scheme 2. Enantiopure starting materials for this work were obtained *via* multistep syntheses starting from the commercially available, enantiopure (*R*)-BINOL, and they were chemically transformed under nonracemizing conditions.¹⁴ Diphosphonate (*R*)-3 was obtained from known enantiopure dibromide (*R*)-5 *via* the Arbuzov reaction, and isolated in pure form by column chromatography. Reaction of (*R*)-3 with commercially-available 4-pyridylaldehyde 6 gave compound (*R*)-7 using standard HWE conditions (THF, *t*-ButOK). The compound was obtained as a mixture of diastereoisomers, with *ca.* 15% of the *cis* stereoisomer present, which we were not able to purify further by standard chromatography. The obtainment of a nontrivial quantity of the more sterically congested *cis* stereoisomer might be rationalized by the fact that the electron-withdrawing pyridine moiety, can stack, in this configuration, over the π -rich binaphthyl unit. Elongation of the π -bridge was carried out making use of the acetal-protected phosphonate 8, which gave



Scheme 1 Retrosynthetic approaches to the synthesis push-pull π -extended binaphthyls through HWE olefination.





Scheme 2 Synthesis of the molecular modules.

the extended pyridyl synthon **9** by HWE with 4-pyridylaldehyde **6**. Small amount of *cis* stereoisomer could in this case be easily separated by standard chromatography. After deprotection under mild acidic conditions, elongated aldehyde **10** was obtained and used without further purifications. Finally, double HWE olefination between **3** and **10** gave stereopure compound (*R*)-**11** in excellent yields. It was fully characterized by ^1H , ^{13}C and 2D NMR spectroscopies and mass spectrometry.

The ^1H NMR spectrum of compound (*R*)-**11** is shown in Fig. 2 (top). The NMR analysis demonstrated that the double substitution occurred efficiently and confirmed that, within the limit of detection of the NMR technique, both newly formed carbon-carbon double bonds in compound (*R*)-**11** are in the *trans* configuration exclusively (with $^3J_{\text{HH}}$ coupling constants of *ca.* 16 Hz).

The attribution of the signals related to the vinyl protons was made possible especially by evaluation of the HETCOR 2D NMR experiment, allowing us to assign the peaks and calculate the values of the coupling constants, which are essential to discriminate between *cis* and *trans* disubstituted carbon-carbon double bonds (Fig. S1†).

The lowest energy conformation (Fig. 2, bottom) for molecule (*R*)-**11**, obtained by molecular modelling calculations (see below), display an almost perfectly C_2 symmetrical structure, with a dihedral angle between the two naphthyl least-squares planes of 85.6° . Interestingly, the conjugated fragments (pyridine-double bond-phenylene-double bond) extending from the 3,3' positions are fully coplanar, but such planar system is significantly out of the plane of the naphthyl unit to

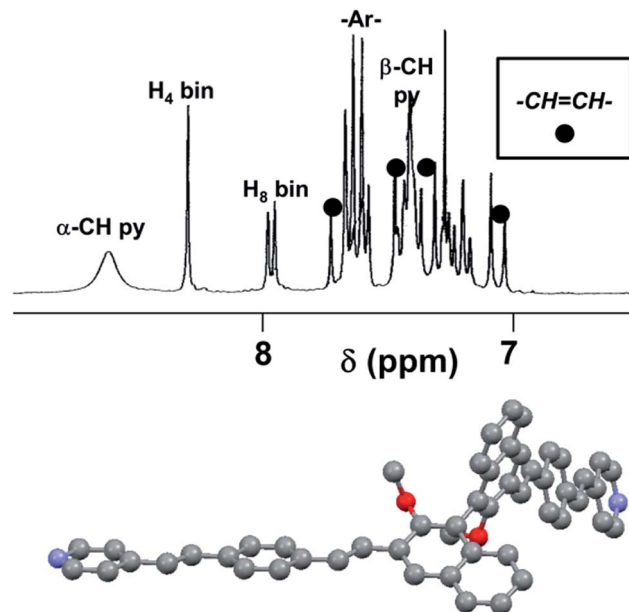


Fig. 2 Top: Partial ^1H NMR spectrum (CDCl_3 , 300 MHz, 25°C ; aromatic region) of compound (*R*)-**11**. Selected peaks are assigned. Bottom: Ball-and-stick rendering of the lowest energy conformation of compound (*R*)-**11** (H atoms omitted for clarity).

which it is bonded (dihedral angle equal to 31.0°), owing to the steric effects of the neighbouring OCH_3 groups in the 2,2' positions of the binaphthyl skeleton.

The NMR signal at 8.6 ppm (Fig. 2 top), related to the α -pyridyl protons, and, to a lesser extent, the signal at 7.4 ppm, related to the β -pyridyl protons, are broad, indicating that one or more dynamic processes are in place, becoming slow on the NMR timescale at this temperature and for this instrument operational frequency (300 MHz).¹⁵ The processes must exchange the positions of the *internal* and *external* α -pyridyl protons, so that they are not anymore equivalent by symmetry. These processes can be in principle due to either: (a) the libration of the pyridine fragments around their own main aryl axis, or (b) the rotation of the entire conjugated fragments (pyridine-double bond-phenylene-double bond) around the neighbouring OCH_3 groups, that is, from top to bottom with respect to the naphthyl plane.^{16,17}

Optical and chiroptical characterization of the supramolecular polarization using Pd^{2+}

The coordination of the difunctional ligand (*R*)-**11** with Pd^{2+} was monitored by means of a full titration of the compound with $\text{Pd}(\text{MeCN})_2\text{Cl}_2$. This Pd^{2+} salt has been previously reported for the formation of complexes in which two pyridine functionalities displace the labile nitrile ligands to form *trans*-tetra-coordinate, square-planar complexes.¹⁸ It is fully soluble in polar organic solvents (MeCN, DMF). The UV-vis titration in MeCN is shown in Fig. 3 (top). The shift of the λ_{max} of the ligand (365 nm), attributed to the π - π^* transition, towards longer wavelengths (381 nm), is in agreement with a coordination of the transition metal cation to the pyridine nitrogen atoms, and



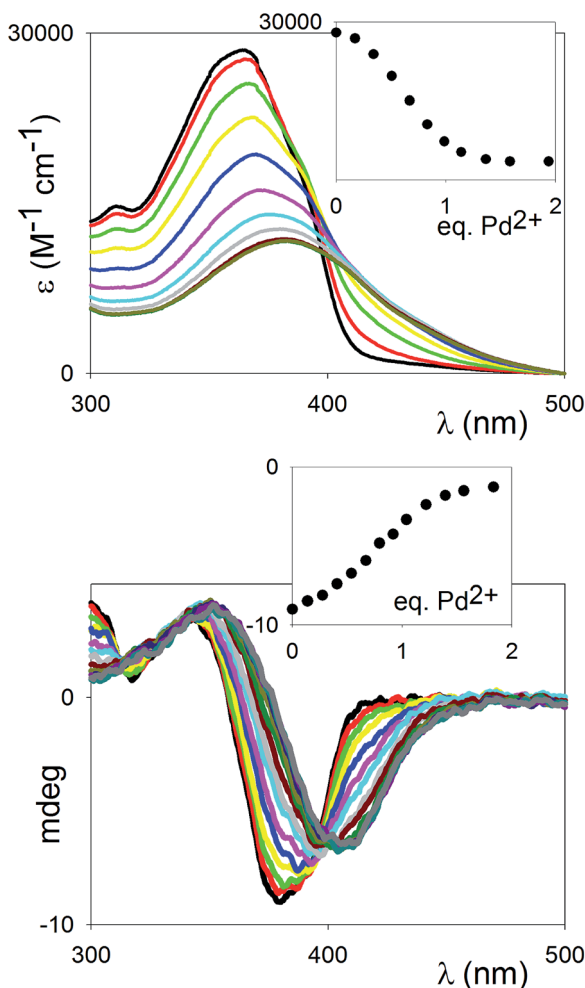


Fig. 3 Top: UV titration of ligand (*R*)-**11** (6.65×10^{-5} M) with $\text{Pd}(\text{MeCN})_2\text{Cl}_2$ in MeCN at 25 °C. Inset: titration profile vs. Pd^{2+} added equivalents at 365 nm. Bottom: CD titration of compound (*R*)-**11** (0.77×10^{-5} M) with $\text{Pd}(\text{MeCN})_2\text{Cl}_2$ in MeCN at 25 °C. Inset: titration profile vs. Pd^{2+} added equivalents at 380 nm.

thus a further polarization of the “push–pull” system. The observed stoichiometry at saturation (1 : 1 ligand vs. Pd^{2+}) matches with the complete incorporation of the pyridine moieties (two per ligand) into the Pd^{2+} complexes. The behaviour of the binding profile (inset in Fig. 3, top) is sigmoidal, which is not only indicative of multiple equilibria, but also generally associated with positive cooperativity.¹⁹ It is likely that the multiple equilibria in play involve the formation of both oligomeric and cyclic species (see below, NMR titration).

A titration experiment in DMF essentially confirmed the behavior observed in MeCN, and differences were found only in the relative intensities of the π – π^* band of the free and complexed ligands.

The titration was also monitored by CD spectroscopy (Fig. 3, bottom): an intense exciton couplet signal, classical signature of binaphthyl compounds and due to the two naphthyl chromophores oriented essentially perpendicular to each other, could be observed, with the inversion point corresponding to the λ_{max} of the ligand. The exciton couplet shift towards longer

wavelengths upon complexation, and the signal change saturates at *ca.* 1 eq., in close parallel to the UV-vis titration. The symmetry of the couplet, in terms of intensities of the lowest and highest energy branches, is maintained throughout the titration, pointing to the dominant presence of either uncomplexed or symmetrically dimerized species at every stage of the titration, supporting that a highly cooperative binding behaviour is in play.

In order to examine the coordination behavior further, and to confirm the formation of a linear coordination polymer rather than dimeric or oligomeric cyclic species, a ^1H NMR titration was performed. The titration could not be made in CD_3CN , since using this solvent an insoluble aggregate was formed at the concentrations needed for ^1H NMR measurements (at least 10^{-3} M, two orders of magnitude higher than the UV titrations). Upon addition of Pd^{2+} (*R*)-**11** in DMF, instead, the aggregate species was completely soluble. The NMR spectra for the titration in d_7 -DMF are reported in Fig. S2;† general broadening of the signals is observed, with no further changes observed after the addition of 1 eq. of Pd^{2+} , in agreement with the proposed formation of a coordination polymer *via* pyridine trans coordination to the Pd^{2+} center. The formation of small quantities of cyclic species, however, cannot be completely ruled out.

Linear and nonlinear optical switching behavior by protonation–deprotonation reaction

The UV-vis absorption spectrum of compound (*R*)-**11** in CHCl_3 , displays one major band at 367 nm. This band is essentially unshifted in a polar solvent such as CH_3CN . By comparison, λ_{max} for 6,6'-disubstituted binaphthyls such as compounds **1** and **2**, bearing irreversibly alkylated pyridine nitrogen, is red shifted to a substantial extent (Table 1).

The possibility of switching the optical properties of (*R*)-**11** *via* protonation/deprotonation is clearly illustrated in Fig. 4. Upon exposure of the CHCl_3 solution of (*R*)-**11** to HCl vapors, the absorption maximum is shifted to 414 nm, a red-shift that can be attributed to protonation of the pyridine moiety with formation of (*R*)-**11**·2HCl, in agreement with the red shift observed for the (*R*)-**11**· PdCl_2 complex. The shift is however considerably larger for the protonated system (47 vs. 16 nm).

The reverse transformation can be induced by treatment of the solution with NH_3 vapors, as confirmed by absorption

Table 1 Optical absorption properties for (*R*)-**11**, and (*R*)-**11** protonated and complexed in different solvents, compared with previously reported dyes (*R*)-**1** and (*R*)-**2**

Compound	λ_{max} MeCN (ϵ)	λ_{max} CHCl_3
11	365 (29 000)	367
11 ·2HCl	—	414
11 · PdCl_2	381 (19 000)	—
1 ^a	—	397
2 ·2I ^b	460 (41 800)	—

^a Data taken from ref. 6. ^b Data taken from ref. 7.



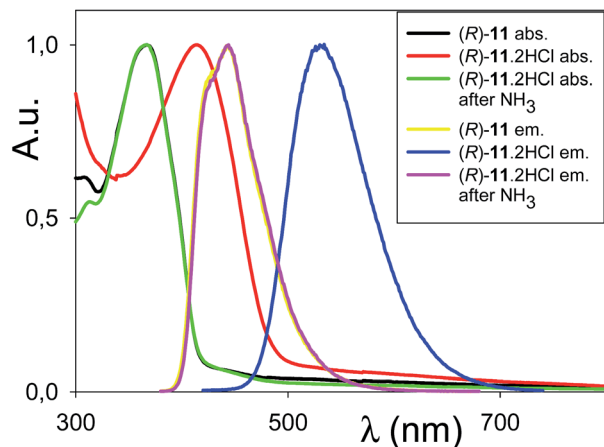


Fig. 4 Normalized absorption and emission spectra in CHCl_3 of (*R*)-**11**, (*R*)-**11**·2HCl and (*R*)-**11**·2HCl after exposure to NH_3 vapors.

spectroscopy. Interestingly, the protonation–deprotonation process is accompanied by a macroscopic variation in the emissive behaviour. In fact, (*R*)-**11** in CHCl_3 displays an intense emission centred at 444 nm which is shifted to 534 nm upon exposure to HCl and restored after treatment with NH_3 vapors. A similar interconversion process can be induced by exposure of solid (*R*)-**11** to HCl and ammonia vapors. The initial 560 nm emission of (*R*)-**11** powder is, in fact, shifted to 600 nm after exposure to HCl vapors and restored by treatment with ammonia vapors (Fig. S3†).

The observation of a 50 nm red-shift of the absorption band upon exposure of the CHCl_3 solution to HCl vapors prompted us to monitor the second-order NLO properties during the (*R*)-**11**/*(R)*-**11**·2HCl interconversion. Hyperpolarizabilities of compounds (*R*)-**11** and (*R*)-**11**·2HCl in CHCl_3 were measured at 1907 nm by electric field-induced second harmonic generation (EFISH)²⁰ and the values are summarized in Table 2.

A higher second-order NLO response of (*R*)-**11**·2HCl with respect to (*R*)-**11** has been obtained in agreement with the observed absorption red-shift. According to DFT and TDDFT calculations on the doubly protonated form of (*R*)-**11** (see below, Computational studies), the modest variation of the dipole moment from the ground to the excited state of (*R*)-**11**·2HCl is not responsible for its observed high second order NLO response compared to (*R*)-**11**, which should be instead attributed to both the red shift of the absorption band and the increased oscillator strength. The solid-state interconversion between (*R*)-**11** and (*R*)-**11**·2HCl was also monitored by means of the Kurtz–Perry powder method²¹ at the non-resonant wavelength of 1907 nm. Powdered batches of (*R*)-**11** and (*R*)-**11**·2HCl showed SHG efficiency respectively equal and 0.7 times that of standard urea. Low SHG signals for powders, with concomitant high SHG values

observed in solution, have been recorded for other binaphthyl residues⁶ and must be associated with an unfavourable anti-parallel or close to antiparallel dipole orientation in the solid state, which is presumably enhanced upon bisprotonation.

Computational studies

DFT and TDDFT calculations on (*R*)-**11** in CHCl_3 provided two $\pi \rightarrow \pi^*$ excitations at 359 and 357 nm, presenting very high oscillator strengths ($f = 2.8$ and 1.6, respectively). The former peak is associated principally with HOMO–1 \rightarrow LUMO and HOMO \rightarrow LUMO+1 transitions, and the latter to HOMO \rightarrow LUMO and HOMO–1 \rightarrow LUMO+1 transitions (see ESI† for a plot of the frontier orbitals). Both pairs of HOMOs and LUMOs are characterized by similar energies but different localization schemes, with HOMO–1 and LUMO+1 more localized on one naphthyl moiety of the molecule, and HOMO and LUMO more localized on the other moiety. As a result, owing to almost symmetrical charge transfers involved in the transitions from one naphthyl moiety to the other one, both absorption peaks are globally characterized by a small charge transfer, as evidenced by a modest increase of the dipole moment from the ground state ($\mu_g = 5.33$ D) to the excited states ($\mu_e = 6.56$ and 7.03 D for the first and second peak, respectively).

The absorption band of (*R*)-**11**·2HCl was well reproduced by DFT and TDDFT calculations on the doubly protonated form of (*R*)-**11** in CHCl_3 , with two $\pi \rightarrow \pi^*$ excitations at 412 and 409 nm ($f = 3.0$ and 1.4, respectively), very similar in character to those obtained for the neutral compound although characterized by individual transitions with much larger charge transfer (see ESI†). The almost symmetrical charge transfers involved in the transitions from one naphthyl moiety to the other one determine a very small variation of the dipole moment from the ground state ($\mu_g = 38.47$ D) to the excited states ($\mu_e = 34.18$ and 34.34 D for the first and second peak, respectively).

CPKS calculations in CHCl_3 reproduced well the hyperpolarizability tensor β trend of the neutral and the doubly protonated forms of (*R*)-**11**. The vector components along the respective dipole directions were $\beta = 106$ and 880×10^{-30} esu, respectively. It is interesting to compare the computed hyperpolarizability of (*R*)-**11** with that of the hypothetical 6,6'-disubstituted compound, analogous to **1** and **2** but functionalized in the same way as (*R*)-**11**. CPKS calculations in CHCl_3 provided significantly increased hyperpolarizability values ($\beta = 328$ and 1540×10^{-30} esu for the neutral and the doubly protonated forms, respectively). Such enhancement should be ascribed to the increased extension of the π -electron delocalized system. In fact, while the dihedral angle between the two naphthyl least-squares planes of this hypothetical compound, 81.5° , was quite similar to that of (*R*)-**11**, the conjugated fragment (pyridine–double bond–phenylene–double bond) bonded to the 6,6' position was essentially coplanar to the naphthyl unit (dihedral angle equal to 5.1°).

Table 2 Nonlinear optical properties of **11** and **11**·2HCl in solution

Compound	<i>C</i> (M)	$\mu\beta$ in CHCl_3 ($\times 10^{-48}$ esu)
11	10^{-3}	170
11 ·2HCl	10^{-4}	2000

Conclusions

We have reported on push–pull binaphthyls of novel conception, in which the π -bridge, bearing at its “pull” end a pyridine



unit, extends from the 3,3'-binaphthyl skeleton, bearing alkoxy "push" unit in the 2,2' positions. These innovative dyes are *chiral*, securing NLO response, and *polarizable* through protonation or a coordination event. The HWE olefination methodology has been an efficient tool for the construction of extended, enantiopure binaphthyl derivatives with high isolated yields. The presence of the terminal pyridine units gives the possibility of further polarizing the system, either by weak coordination with a transition metal, or by reversible protonation. In both cases, the observed shift towards lower energies of the absorption major band indicates that the degree of additional polarization achieved is significant. CD spectroscopy helped to elucidate this very highly active CD chromophore, whose characteristic CD couplet shifts in intensity but not in symmetry, as to indicate complete saturation of the coordinating nitrogen atoms of the pyridine ligands. The EFISH values for the system are remarkable, when compared with those obtained for similar systems reported in the literature.

Experimental section

General experimental

All available compounds were purchased from commercial sources and used as received. Compounds (*R*)-5 (ref. 22) and **8** (ref. 23) were prepared as previously described. THF (Na, benzophenone), Et₂O (Na, benzophenone) and CH₂Cl₂ (CaH₂) were dried and distilled before use. ¹H and ¹³C NMR spectra were recorded from solutions in CDCl₃ on Bruker 200 or AMX300 with the solvent residual proton signal as a standard. Analytical thin layer chromatography was performed on silica gel, chromophore loaded, commercially available plates. Flash chromatography was carried out using silica gel (pore size 60 Å, 230–400 mesh). ¹H and ¹³C NMR spectra were recorded from solutions in CDCl₃ on 200–300 MHz or 500 MHz spectrometer with the solvent residual proton signal or tetramethylsilane as a standard. The UV-vis spectroscopic studies were recorded using commercially-available spectrophotometers. Mass spectra were recorded using an electrospray ionization instrument (ESI). Optical rotations were measured on a polarimeter in a 10 cm cell with a sodium lamp (λ = 589 nm) and are reported as follows: [α]_D²⁵ (c = mg (mL)^{−1}, solvent). CD spectra were recorded at 25 °C at a scanning speed of 50 nm min^{−1} and were background corrected. Each spectrum is the instrument average of four consecutive scans. Mass spectra were recorded using an electrospray ionization instrument.

Compound (R)-3. A solution of compound (*R*)-5 (415 mg, 0.83 mmol) and triethyl phosphite (6.9 g, 41.5 mmol, 50 eq.) was refluxed in toluene (30 mL) for 24 h. After cooling, the solvent and excess phosphite were removed *in vacuo*, and the product was purified by flash chromatography (SiO₂; hexane/AcOEt to remove the excess triethyl phosphite, then AcOEt/MeOH 100/0 to 95/5), to yield compound (*R*)-3 as a yellow oil (386 mg, 76%). [α]_D²⁵ = −26.0° (c = 0.003, CH₂Cl₂). ¹H-NMR (300 MHz, CDCl₃) δ = 8.11 (d, 2H; binaphthyl), 7.88 (d, 2H; binaphthyl), 7.39 (t, 2H; binaphthyl), 7.28–7.13 (m, 4H; binaphthyl), 4.13 (m, 8H; PO(OCH₂CH₃)₂), 3.59 (m, 4H; ArCH₂PO(OEt)₂), 3.29 (s, 6H; OCH₃), 1.31 (m, 12H; P(O)(OCH₂CH₃)₂). ¹³C-NMR

(75 MHz, CDCl₃): δ = 154.8 (C_q), 133.5 (C_q), 130.8 (CH), 130.2 (C_q), 127.7 (CH), 126.1 (CH), 125.5 (CH), 125.2 (C_q), 124.8 (CH), 124.3 (C_q), 62.0 (CH₂), 60.7 (OCH₃), 28.0 (PO(OCH₂CH₃)₂), 26.2 (PO(OCH₂CH₃)₂), 16.4 (PO(OCH₂CH₃)₂), 16.3 (PO(OCH₂CH₃)₂). This compound has already been prepared through a different route.²⁴

Compound (R)-7. *t*-BuOK (73 mg, 0.65 mmol) was added to a solution of compound **6** (35 mg, 0.33 mmol) and compound (*R*)-5 (50 mg, 0.08 mmol) in dry THF (25 mL) at 0 °C. After stirring at room temperature for 15 h, THF was removed *in vacuo* and H₂O (50 mL) was added. The mixture was extracted with CH₂Cl₂ (3 × 30 mL) and the organic phase was dried (Na₂SO₄). Purification of the reaction mixture by flash chromatography (SiO₂; AcOEt/*i*-PrOH 100/0 to 98/2) afforded (*R*)-7 as an inseparable mixture of *cis* and *trans* stereoisomers (26 mg, 62%). MS(ESI): *m/z* 521 ([M]⁺, 100%), 1063 ([2M + Na]⁺, 10%). ¹H NMR (CDCl₃, 300 MHz, 25 °C) δ = 8.64 (d, 4H; –ArH– pyridine *trans* stereoisomer), 8.51 (d, –ArH– pyridine minor stereoisomer, *ca.* 15%), 8.31 (s, 2H; binaphthyl), 7.98 (d, 2H; binaphthyl), 7.84 (d, 2H; –CH– vinyl, *J* = 16 Hz), 7.48–7.18 (m, 12H; binaphthyl and pyridine and –CH– vinyl), 3.47 (s, –OCH₃ minor stereoisomer), 3.45 (s, 6H; –OCH₃). The *trans* isomer, synthesized through Heck coupling from 3,3'-diiodo-2,2'-dimethoxy-1,1'-binaphthyl and 4-vinylpyridine has already been published²⁵ but the NMR data have not been reported.

Compound 9. *t*-BuOK (418 mg, 3.74 mmol) was added to a solution of pyridylaldehyde **1** (100 mg, 0.93 mmol) and compound **2** (309 mg, 0.93 mmol) in dry THF (50 mL) at 0 °C. After stirring at room temperature for 15 h, THF was removed *in vacuo* and H₂O (50 mL) was added. The mixture was extracted with CH₂Cl₂ (3 × 50 mL) and the organic phase was dried (Na₂SO₄). Purification of the reaction mixture by flash chromatography (SiO₂; hexane/ethyl acetate gradient from 100/0 to 8/2) afforded *cis* **9** (eluting first, 26 mg, 10%) and *trans* **9** (eluting second, 146 mg, 55%). ¹H NMR (CDCl₃, 200 MHz, 25 °C) for *cis* δ = 8.47 (bs, 2H; pyridine), 7.52–7.13 (m, 6H; –ArH– and pyridine), 6.78 (d, 2H; –CH– vinyl, *J* = 11 Hz), 6.50 (d, 2H; –CH– vinyl, *J* = 11 Hz), 5.49 (s, 1H; –CH(OEt)₂), 3.59 (m, 4H; –OCH₂CH₃), 1.25 (t, 6H; –OCH₂CH₃). For *trans* δ = 8.58 (d, 2H; pyridine), 7.53 (m, 4H; –ArH–), 7.36 (m, 3H; –ArH– pyridine and –CH– vinyl), 7.16 (d, 2H; –CH– vinyl, *J* = 16 Hz), 5.53 (s, 1H; –CH(OEt)₂), 3.60 (m, 4H; –OCH₂CH₃), 1.26 (t, 6H; –OCH₂CH₃).

Compound 10. HCl 1 M (3 mL) was added to a solution of *trans* **9** (146 mg, 0.52 mmol) in CHCl₃ (115 mL). After 1 h of stirring at room temperature, a saturated NaHCO₃ aqueous solution was added (120 mL). The organic layer was separated, and the aqueous layer was extracted with CH₂Cl₂ (3 × 100 mL), the organic layers combined and dried (Na₂SO₄) to yield, after solvent removal, compound **10** (100 mg, 92%) which was used without further purification. ¹H NMR (CDCl₃, 200 MHz, 25 °C) δ = 10.04 (s, 1H; –CHO), 8.64 (d, 2H; pyridine), 7.93 (d, 2H; –ArH–), 7.71 (d, 2H; –ArH–), 7.43–7.00 (m, 4H; –ArH– pyridine and –CH– vinyl). This compound has been reported in the literature but no experimental details or characterization has been given.²⁶

Compound (R)-11. *t*-BuOK (107 mg, 0.96 mmol) was added to a solution of compound **10** (100 mg, 0.48 mmol) and compound



(*R*)-3 (147 mg, 0.24 mmol) in dry THF (25 mL) at 0 °C. After stirring at room temperature for 15 h, THF was removed *in vacuo* and H₂O (50 mL) was added. The mixture was extracted with CH₂Cl₂ (3 × 30 mL) and the organic phase was dried (Na₂SO₄). Purification of the reaction mixture by flash chromatography (SiO₂; hexane/ethyl acetate 2/8) afforded stereopure (*R*)-11 (127 mg, 73%). [α]_D²⁵ = −489° (*c* = 0.0022, CH₂Cl₂). MS(ESI): *m/z* 725 ([M + H]⁺, 100%). ¹H NMR (CDCl₃, 300 MHz, 25 °C) δ = 8.60 (bs, 4H; −ArH− pyridine), 8.31 (s, 2H; binaphthyl), 7.96 (d, 2H; binaphthyl), 7.70 (d, 2H; −CH− vinyl, *J* = 16 Hz), 7.62 (m, 8H; −ArH−), 7.48–7.38 (m, 8H; pyridine, binaphthyl and −CH− vinyl), 7.35 (d, 2H; CH− vinyl, *J* = 16 Hz), 7.28 (t, 2H; binaphthyl), 7.21 (t, 2H; binaphthyl), 7.07 (d, 2H; CH− vinyl, *J* = 16 Hz), 3.46 (s, 6H; −OCH₃). ¹³C NMR (CDCl₃, 75 MHz, 25 °C) δ = 154.4 (C_q), 150.0 (CH), 144.6 (C_q), 138.2 (C_q), 135.5 (C_q), 133.7 (C_q), 132.7 (CH), 130.8 (C_q), 129.8 (CH), 128.1 (CH), 127.4 (CH), 127.0 (CH), 126.3 (CH), 126.2 (CH), 125.7 (CH), 125.6 (CH), 125.1 (CH), 124.6 (CH), 120.7 (CH), 61.2 (OCH₃).

Procedure for NMR, UV and CD titrations

The titration experiments were conducted as follows: to a stock solution of chromophore (*R*)-11 (solution A) were added several aliquots of the Pd²⁺ salt (solution B). Solution B is formed by the Pd²⁺ salt (at higher concentration) dissolved in solution A, in order to maintain one species always at the same, constant concentration.

Absorption and emission spectroscopy

Electronic absorption spectra were obtained using a Jasco V-530 spectrophotometer. Photoluminescence (PL) measurements were obtained with a SPEX 270 M monochromator equipped with a N₂ cooled charge-coupled device exciting either with a monochromated Xe lamp or an Ar⁺ laser. The spectra were corrected for the instrument response.

NLO measurements

EFISH measurements were carried out in CHCl₃ and DMF solutions at the concentrations specified in Table 2, at a nonresonant fundamental wavelength of 1907 nm using a Q-switched, mode-locked Nd³⁺:YAG laser. The 1064 nm initial wavelength was shifted to 1907 nm by a Raman shifter with a high-pressure H₂ cell.

Computational details

The molecular structures of (*R*)-11, its bisprotonated form and the analogous 6,6'-disubstituted compounds have been optimized in CHCl₃ within the DFT approach, using the PBE0 functional^{27,28} which has previously been judged well suited for describing the electronic features of a series of organic dyes.²⁹ The 6-311G** basis set was chosen for all atoms. Solvent effects have been taken into account using the conductor-like polarizable continuum model, CPCM.³⁰ Using the PBE0/6-311G** optimized geometries, standard vertical Time Dependent DFT (TDDFT) calculations^{31–33} have been carried out at

the TD- ω B97X/6–311++G** level using the so-called non-equilibrium approach, to determine the absorption wavelengths. The ω B97X³⁴ functional was found to provide the better agreement with the experimental results with respect to other tested functionals (PBE0 and M062X), which gave too high excitation energies in particular for the bisprotonated form. Hyperpolarizabilities have been computed at the same frequency as used in the experiment, using the Coupled Perturbed Kohn Sham (CPKS) approach with the CAM-B3LYP functional,³⁵ which was recently recommended for hyperpolarizability calculations of midsize organic chromophores.³⁶ The reported hyperpolarizability values include the 1/2 factor to be compared with the experimental results. All calculations have been performed with the Gaussian suite of programs.³⁷

Acknowledgements

Support from the University of Pavia, MIUR (Programs of National Relevant Interest PRIN grants 2004-033354 and 2009-A5Y3N9), and, from CARIPLO Foundation (2007–2009) and, in part, from INSTM-Regione Lombardia (2010–2012 and 2013–2015) is gratefully acknowledged. D.P. wishes to thank Dr Arvind K. Sharma for experimental assistance, and Prof. Mariella Mella for performing the HETCOR NMR experiment.

Notes and references

- 1 A. C. Grimsdale, K. L. Chan, R. E. Martin, P. G. Jokisz and A. B. Holmes, *Chem. Rev.*, 2009, **109**, 897–1091.
- 2 (a) S. R. Marder, *Chem. Commun.*, 2006, 131–134; (b) P. A. Sullivan and L. R. Dalton, *Acc. Chem. Res.*, 2010, **43**, 10–18; (c) H. Kang, A. Facchetti, H. Jiang, E. Cariati, S. Righetto, R. Ugo, C. Zuccaccia, A. Macchioni, C. L. Stern, Z. Liu, S. T. Ho, E. C. Brown, M. A. Ratner and T. J. Marks, *J. Am. Chem. Soc.*, 2007, **129**, 3267–3286.
- 3 (a) P. Jonkheijm, P. van der Schoot, A. P. H. J. Schenning and E. W. Meijer, *Science*, 2006, **313**, 80–83; (b) T. Verbiest, S. Van Elshocht, M. Kauranen, L. Hellemans, J. Snauwaert, C. Nuckolls, T. Katz and A. Persoons, *Science*, 1998, **282**, 913–915.
- 4 (a) M. Caricato, A. K. Sharma, C. Coluccini and D. Pasini, *Nanoscale*, 2014, 7165–7174; (b) A. Shockravi, A. Javadi and E. Abouzari-Lotf, *RSC Adv.*, 2013, **3**, 6717–6746.
- 5 (a) H.-J. Deussen, E. Hendrickx, C. Boutton, D. Krog, K. Clays, K. Bechgaard, A. Persoons and T. Bjørnholm, *J. Am. Chem. Soc.*, 1996, **118**, 6841–6852; (b) G. Koeckelberghs, M. Vangheluwe, I. Picard, L. De Groof, T. Verbiest, A. Persoons and C. Samyn, *Macromolecules*, 2004, **37**, 8530–8537; (c) P. Yan, A. C. Millard, M. Wei and L. M. Loew, *J. Am. Chem. Soc.*, 2006, **128**, 11030–11031; (d) G. Koeckelberghs, T. Verbiest, M. Vangheluwe, L. De Groof, I. Asselberghs, I. Picard, K. Clays, A. Persoons and C. Samyn, *Chem. Mater.*, 2005, **17**, 118–121; (e) D. Cornelis, E. Franz, I. Asselberghs, K. Clays, T. Verbiest and G. Koeckelberghs, *J. Am. Chem. Soc.*, 2011, **133**, 1317–1327; (f) G. Yang, Y. Sib and Z. Su, *Org. Biomol. Chem.*, 2012, **10**, 8418–8425.



- 6 H.-J. Deussen, C. Boutton, N. Thorup, T. Geisler, E. Hendrickx, K. Bechgaard, A. Persoons and T. Bjørnholm, *Chem.-Eur. J.*, 1998, **4**, 240–250.
- 7 B. J. Coe, E. C. Harper, K. Clays and E. Franz, *Dyes Pigm.*, 2010, **87**, 22–29.
- 8 For supramolecularly polarizable π -conjugated systems: (a) D. T. McQuade, A. E. Pullen and T. M. Swager, *Chem. Rev.*, 2000, **100**, 2537–2574; (b) G. R. Whittell, M. D. Hager, U. S. Schubert and I. Manners, *Nat. Mater.*, 2011, **10**, 176–188; (c) F. Wurthner, J. Schmidt, M. Stolte and R. Wortmann, *Angew. Chem., Int. Ed.*, 2006, **45**, 3842–3846; (d) G. Fabbrini, E. Menna, M. Maggini, A. Canazza, G. Marcolongo and M. Meneghetti, *J. Am. Chem. Soc.*, 2004, **126**, 6238–6239; (e) A. J. Zuccherro, P. L. McGrier and U. H. F. Bunz, *Acc. Chem. Res.*, 2010, **43**, 397–408.
- 9 E. Cariati, A. Forni, S. Biella, P. Metrangolo, F. Meyer, G. Resnati, S. Righetto, E. Tordin and R. Ugo, *Chem. Commun.*, 2007, 2590–2592.
- 10 (a) E. Cariati, C. Botta, S. Danelli, A. Forni, A. Giaretta, U. Giovanella, E. Lucenti, D. Marinotto, S. Righetto and R. Ugo, *Chem. Commun.*, 2014, 14225–14228; (b) E. Cariati, C. Dragonetti, E. Lucenti, F. Nisic, S. Righetto, D. Roberto and E. Tordin, *Chem. Commun.*, 2014, 1608–1610.
- 11 (a) C. Gütz, R. Hovorka, C. Stobe, N. Struch, F. Topić, G. Schnakenburg, K. Rissanen and A. Lützen, *Eur. J. Org. Chem.*, 2014, 206–216; (b) C. Gütz, R. Hovorka, C. Stobe, N. Struch, J. Bunzen, G. Meyer-Eppler, Z.-W. Qu, S. Grimme, F. Topić, K. Rissanen, M. Cetina, M. Engeser and A. Lützen, *J. Am. Chem. Soc.*, 2014, **136**, 11830–11838; (c) C.-D. Wu and W. Lin, *Inorg. Chem.*, 2005, 1178–1180; (d) Y. Cui, H. L. Ngo and W. Lin, *Chem. Commun.*, 2003, 1388–1389; (e) C.-D. Wua and W. Lin, *Dalton Trans.*, 2006, 4563–4569.
- 12 (a) A. Bencini, C. Coluccini, A. Garau, C. Giorgi, V. Lippolis, L. Messori, D. Pasini and S. Puccioni, *Chem. Commun.*, 2012, **48**, 10428–10430; (b) C. Coluccini, D. Dondi, M. Caricato, A. Taglietti, M. Boiocchi and D. Pasini, *Org. Biomol. Chem.*, 2010, **8**, 1640–1649; (c) M. Caricato, N. J. Leza, K. Roy, D. Dondi, G. Gattuso, L. S. Shimizu, D. A. Vander Griend and D. Pasini, *Eur. J. Org. Chem.*, 2013, 6078–6083; (d) M. Caricato, A. Olmo, C. Gargiulli, G. Gattuso and D. Pasini, *Tetrahedron*, 2012, **68**, 7861–7866; (e) M. Caricato, C. Coluccini, D. Dondi, D. A. VanderGriend and D. Pasini, *Org. Biomol. Chem.*, 2010, **8**, 3272–3280; (f) A. Moletti, C. Coluccini, D. Pasini and A. Taglietti, *Dalton Trans.*, 2007, 1588–1592; (g) C. Coluccini, A. Mazzanti and D. Pasini, *Org. Biomol. Chem.*, 2010, **8**, 1807–1815; (h) S. Colombo, C. Coluccini, M. Caricato, C. Gargiulli, G. Gattuso and D. Pasini, *Tetrahedron*, 2010, **66**, 4206–4211; (i) A. Pacini, M. Caricato, S. Ferrari, D. Capsoni, A. Martínez de Ilarduya, S. Muñoz-Guerra and D. Pasini, *J. Polym. Sci., Part A: Polym. Chem.*, 2012, **50**, 4790–4799; (j) M. Caricato, S. Díez González, I. Arandia Ariño and D. Pasini, *Beilstein J. Org. Chem.*, 2014, **10**, 1308–1316; (k) M. Caricato, N. J. Leza, C. Gargiulli, G. Gattuso, D. Dondi and D. Pasini, *Beilstein J. Org. Chem.*, 2012, **8**, 967–976; (l) M. Agnes, A. Sorrenti, D. Pasini, K. Wurst and D. B. Amabilino, *CrystEngComm*, 2014, **16**, 10131–10138; (m) M. Crespo Alonso, M. Arca, F. Isaia, R. Lai, V. Lippolis, S. K. Callear, M. Caricato, D. Pasini, S. J. Coles and M. C. Aragoni, *CrystEngComm*, 2014, **16**, 8582–8590; (n) M. Caricato, A. Deforge, D. Bonifazi, D. Dondi, A. Mazzanti and D. Pasini, *Org. Biomol. Chem.*, 2015, DOI: 10.1039/c4ob02643h.
- 13 (a) C. Coluccini, A. K. Sharma, M. Caricato, A. Sironi, E. Cariati, S. Righetto, E. Tordin, C. Botta, A. Forni and D. Pasini, *Phys. Chem. Chem. Phys.*, 2013, **15**, 1666–1674; (b) M. Caricato, C. Coluccini, D. A. Vander Griend, A. Forni and D. Pasini, *New J. Chem.*, 2013, **37**, 2792–2799; (c) D. Pasini, P. P. Righetti and V. Rossi, *Org. Lett.*, 2002, **4**, 23–26; (d) L. Garlaschelli, I. Messina, D. Pasini and P. P. Righetti, *Eur. J. Org. Chem.*, 2002, 3385–3392; (e) C. Coluccini, P. Metrangolo, M. Parachini, D. Pasini, G. Resnati and P. Righetti, *J. Polym. Sci., Part A: Polym. Chem.*, 2008, **46**, 5202–5213; (f) C. Coluccini, D. Pasini, P. Righetti and D. A. Vander Griend, *Tetrahedron*, 2009, **65**, 10436–10440.
- 14 H. T. Stock and R. M. Kellogg, *J. Org. Chem.*, 1996, **61**, 3093–3105.
- 15 Other 4-pyridyl-vinylene conjugated systems, similarly to compound (R)-**11**, show broad α -pyridyl protons at room temperature. See: C. Stangel, A. Bagaki, P. A. Angaridis, G. Charalambidis, G. D. Sharma and A. G. Coutsolelos, *Inorg. Chem.*, 2014, **53**, 11871–11881.
- 16 The low solubility of compound **11** in appropriate solvents for low temperature NMR analysis (e.g., THF, see ref. 12g) prevented us from a more detailed dynamic of the system. Additionally, a thorough investigation of such dynamic behaviour will require the synthesis of a series of model compounds (such as the naphthyl analogue of compound **11**, in which the chiral axis is not present) and not, which is outside the purpose of this paper.
- 17 The exchange method allows to calculate values for the rate constant k_{ex} of the exchange process from NMR analysis, J. Sandström, *Dynamic NMR Spectroscopy*, Academic Press, London, 1982, ch. 6, from the approximate expression $k_{\text{ex}} = \pi(\Delta\nu)$, where $\Delta\nu$ is the difference (Hz) between the line width at the temperature T_{ex} , where exchange of sites occurs, and the line width in the absence of exchange (which in our case was assumed the value of the sharp H4-bin signal at 8.3 ppm in Fig. 2). A value of $k_{\text{ex}} = 16$ Hz was calculated in our case, which translates, by employing the Eyring equation, into a $\Delta G^\ddagger = 12$ kcal mol⁻¹ value for the energy barrier.
- 18 For examples of pyridine moieties forming *trans* PdCl₂ coordination complexes, see: (a) Z. Qin, M. C. Jennings and R. J. Puddephatt, *Inorg. Chem.*, 2001, **40**, 6220–6228; (b) L. Pirondini, D. Bonifazi, E. Menozzi, E. Wegelius, K. Rissanen, C. Massera and E. Dalcanele, *Eur. J. Org. Chem.*, 2001, 2311–2320; (c) Y. S. Chong, M. D. Smith and K. D. Shimizu, *J. Am. Chem. Soc.*, 2001, **123**, 7463–7464; (d) M. T. Stone and J. S. Moore, *J. Am. Chem. Soc.*, 2005, **127**, 5928–5935; (e) G. Giachi, M. Frediani, W. Oberhauser and



- E. Passaglia, *J. Polym. Sci., Polym. Chem. Ed.*, 2011, **49**, 4708–4713.
- 19 (a) K. A. Connors, *Binding Constants: The Measurement of Molecular Complex Stability*, Wiley, New York, NY, 1987. See also: (b) G. Fernández, L. Sánchez, E. M. Pérez and N. Martín, *J. Am. Chem. Soc.*, 2008, **130**, 10674–10683; (c) L. D. Byers, *J. Chem. Educ.*, 1977, **54**, 352–354; (d) G. Ercolani, *J. Am. Chem. Soc.*, 2003, **125**, 16097–16103; (e) J. Hamacek and C. Piguet, *J. Phys. Chem. B*, 2006, **110**, 7783–7792.
- 20 (a) D. Roberto, R. Ugo, S. Bruni, E. Cariati, F. Cariati, P. Fantucci, I. Invernizzi, S. Quici, I. Ledoux and J. Zyss, *Organometallics*, 2000, **19**, 1775–1788; (b) I. Ledoux and J. Zyss, *Chem. Phys.*, 1982, **73**, 203–213; (c) K. D. Singer and A. F. Garito, *J. Chem. Phys.*, 1981, **75**, 3572–3580.
- 21 S. K. Kurtz and T. T. Perry, *J. Appl. Phys.*, 1968, **39**, 3798.
- 22 C. Coluccini, A. Castelluccio and D. Pasini, *J. Org. Chem.*, 2008, **73**, 4237–4240.
- 23 C. Coluccini, A. K. Sharma, D. Merli, D. Vander Griend, B. Mannucci and D. Pasini, *Dalton Trans.*, 2011, **40**, 11719–11725.
- 24 R. C. Helgeson, G. R. Weisman, J. R. Toner, T. L. Tarnowski, Y. Chao, J. M. Mayer and D. J. Cram, *J. Am. Chem. Soc.*, 1979, **101**, 4928–4941.
- 25 Y. Cui, H. L. Ngo and W. Lin, *Chem. Commun.*, 2003, 1388–1389.
- 26 M. I. Ranasinghe, P. Murphy, Z. Lu, S. D. Huang, R. J. Twieg and T. Goodson III, *Chem. Phys. Lett.*, 2004, **383**, 411–417.
- 27 M. Ernzerhof and G. E. Scuseria, *J. Chem. Phys.*, 1999, **110**, 5029–5036.
- 28 C. Adamo and V. Barone, *J. Chem. Phys.*, 1999, **110**, 6158–6170.
- 29 (a) D. Jacquemin, E. A. Perpète, G. E. Scuseria, I. Ciofini and C. Adamo, *J. Chem. Theory Comput.*, 2008, **4**, 123–135; (b) D. Jacquemin, V. Wathelet, E. A. Perpète and C. Adamo, *J. Chem. Theory Comput.*, 2009, **5**, 2420.
- 30 V. Barone and M. Cossi, *J. Phys. Chem. A*, 1998, **102**, 1995–2001.
- 31 E. Runge and E. K. U. Gross, *Phys. Rev. Lett.*, 1984, **52**, 997–1000.
- 32 R. E. Stratmann, G. E. Scuseria and M. J. Frisch, *J. Chem. Phys.*, 1998, **109**, 8218–8224.
- 33 M. E. Casida, *J. Mol. Struct.: THEOCHEM*, 2009, **914**, 3–18.
- 34 J. D. Chai and M. Head-Gordon, *J. Chem. Phys.*, 2008, **128**, 084106–084115.
- 35 T. Yanai, D. Tew and N. C. Handy, *Chem. Phys. Lett.*, 2004, **393**, 51–57.
- 36 L. E. Johnson, L. R. Dalton and B. H. Robinson, *Acc. Chem. Res.*, 2014, **47**, 3258–3265.
- 37 M. J. Frisch, *et al.*, *Gaussian 09, Revision D.01*, Gaussian, Inc., Wallingford CT, 2013.

